

Institutionen för systemteknik

Department of Electrical Engineering

Examensarbete

Iris recognition using standard cameras

Examensarbete utfört i Bildkodning
vid Tekniska högskolan i Linköping
av

Hans Holmberg

LITH-ISY-EX--06/3825--SE

Linköping 2006



Linköpings universitet
TEKNISKA HÖGSKOLAN

Department of Electrical Engineering
Linköpings universitet
SE-581 83 Linköping, Sweden

Linköpings tekniska högskola
Linköpings universitet
581 83 Linköping

Iris recognition using standard cameras

Examensarbete utfört i Bildkodning
vid Tekniska högskolan i Linköping
av

Hans Holmberg

LITH-ISY-EX--06/3825--SE

Handledare: **Ingemar Ragnemalm**
ISY, Linköpings universitet

Examinator: **Ingemar Ragnemalm**
ISY, Linköpings universitet

Linköping, 18 September, 2006

 <p>Avdelning, Institution Division, Department Image Coding Group Department of Electrical Engineering Linköpings universitet S-581 83 Linköping, Sweden </p>		Datum Date 2006-09-18
Språk Language <input type="checkbox"/> Svenska/Swedish <input checked="" type="checkbox"/> Engelska/English <input type="checkbox"/> _____	Rapporttyp Report category <input type="checkbox"/> Licentiatavhandling <input checked="" type="checkbox"/> Examensarbete <input type="checkbox"/> C-uppsats <input type="checkbox"/> D-uppsats <input type="checkbox"/> Övrig rapport <input type="checkbox"/> _____	ISBN _____ ISRN LITH-ISY-EX--06/3825--SE
URL för elektronisk version http://www.bk.isy.liu.se/ http://www.ep.liu.se/2006/3825		
Titel Irisigenkänning för standardkameror Title Iris recognition using standard cameras		
Författare Hans Holmberg Author		
Sammanfattning Abstract		
<p>This master thesis evaluates the use of off-the-shelf standard cameras for biometric identification of the human iris. As demands on secure identification are constantly rising and as the human iris provides with a pattern that is excellent for identification, the use of inexpensive equipment could help iris recognition become a new standard in security systems.</p> <p>To test the performance of such a system a review of the current state of the research in the area was done and the most promising methods were chosen for evaluation. A test environment based on open source code was constructed to measure the performance of iris recognition methods, image quality and recognition rate.</p> <p>In this paper the image quality of a database consisting of images from a standard camera is assessed, the most important problem areas identified, and the overall recognition performance measured. Iris recognition methods found in literature are tested on this class of images. These together with newly developed methods show that a system using standard equipment can be constructed. Tests show that the performance of such a system is promising.</p>		
Nyckelord Keywords iris recognition, biometric identification, image processing, computer vision		

Abstract

This master thesis evaluates the use of off-the-shelf standard cameras for biometric identification of the human iris. As demands on secure identification are constantly rising and as the human iris provides with a pattern that is excellent for identification, the use of inexpensive equipment could help iris recognition become a new standard in security systems.

To test the performance of such a system a review of the current state of the research in the area was done and the most promising methods were chosen for evaluation. A test environment based on open source code was constructed to measure the performance of iris recognition methods, image quality and recognition rate.

In this paper the image quality of a database consisting of images from a standard camera is assessed, the most important problem areas identified, and the overall recognition performance measured. Iris recognition methods found in literature are tested on this class of images. These together with newly developed methods show that a system using standard equipment can be constructed. Tests show that the performance of such a system is promising.

Acknowledgements

I would like to thank Ingemar Ragnemalm for letting me realize my idea for this thesis, Adriana for support and love, my family for putting up with the initial iris imaging sessions, the creators of the UBIRIS and the CASIA iris image databases, Libor Masek for his open source code, god and house music. Portions of the research in this paper use the CASIA iris image database collected by Institute of Automation, Chinese Academy of Sciences.

Notation

This section introduces the notation and symbols used in this report.

Symbols

x, y, u, v	Coordinates in \mathbb{R}^2
r, θ	Coordinates in 2D polar space
σ_a^2	Standard deviation of the distribution a
μ_a	Mean of the distribution a

Operators and functions

P^*	Complex conjugate of P
P^t	Transpose of P
$X * Y$	Convolution of X and Y
$A \otimes B$	Binary exclusive or (xor) of A and B

Acronyms

IR	Iris Recognition
SNR	Signal-to-Noise Ratio is a measure of image fidelity
HD	Hamming Distance as defined in section 4.5.1
EER	Equal Error Rate as defined in section 3.1
FAR	False Acceptance Rate as defined in section 3.1
FRR	False Rejection Rate as defined in section 3.1

Contents

1	Introduction	1
1.1	Iris recognition using standard cameras	1
1.2	The purpose of this report	2
1.3	Document structure	2
2	Problem description	3
2.1	Resolution	3
2.2	Occlusion	3
2.3	Noise	4
2.4	Reflections	4
2.5	Compression	5
2.6	Focus	5
2.7	Light level	5
3	Theory	7
3.1	Biometric identification for IR	7
3.2	Image processing for IR	8
3.2.1	Edge detection	9
3.2.2	The Canny operator	9
3.2.3	Orientation in an image	10
3.2.4	The Hough transform	10
4	Iris recognition methods	13
4.1	The IR process	13
4.2	Segmentation	14
4.2.1	Hough transform based methods	15
4.2.2	Daugmans integro-differential operator	15
4.2.3	Methods based on thresholding	16
4.3	Normalization	16
4.4	Mask generation	17
4.5	Encoding and matching	17
4.5.1	Daugmans method	17
4.5.2	Other methods	18
4.6	Proposed new methods	19
4.6.1	Segmentation	19

4.6.2	Mask generation	22
5	Evaluation	25
5.1	The IrisLAB test system	25
5.2	Iris image databases used	28
5.2.1	The UBIRIS database	28
5.2.2	The CASIA database	29
5.3	Tests	29
5.3.1	Encoding parameters	29
5.3.2	Resolution	30
5.3.3	Noise	30
5.3.4	Reflection	32
5.3.5	Occlusion	32
5.3.6	Focus	34
5.3.7	Light	34
5.3.8	Compression	35
5.3.9	Segmentation methods	37
5.3.10	Mask methods	38
5.3.11	Recognition performance	38
6	Discussion	41
6.1	Summary of results	41
6.2	Fulfillment of goals	41
6.3	Future work	42
	Bibliography	43
A	Full test results	45
A.0.1	UBIRIS Encoding parameters	45
A.0.2	Full resolution test results	45

Chapter 1

Introduction

Biometrics is, due to constant demands on higher security, an expanding field and the use of the human iris as a mean of identification has proved to be one of the most promising and secure methods. The iris is, due to its unique biological properties, exceptionally suited for identification; the iris is protected from the environment, stable over time, characteristic in shape and contains a high amount of discriminating information in its pattern. According to a survey [16] done by the National Physical Laboratory in the UK iris recognition (IR) outperforms other biometric identification methods (e.g. fingerprints, voice and face recognition) proving the technology to be the safest.



Figure 1.1. An example of an iris from the UBIRIS database [20]

1.1 Iris recognition using standard cameras

All iris recognition systems found in literature are based on specialized hardware, imaging the eye under favorable conditions. As imaging technology is rapidly becoming cheaper and the quality of off the shelf cameras is constantly rising, the idea behind this thesis is to look into the possibilities of making iris recognition an inexpensive and widespread technology using cheap imaging devices in less restrictive imaging situations.

When imaging the iris under less-than ideal conditions artifacts in the image occur such as different types of noise and reflections from light sources, artifacts that introduce errors in the iris recognition process, influence the performance and must be taken in consideration when designing IR systems.

1.2 The purpose of this report

The purpose of this report is to evaluate the use of standard cameras for IR, localize and grade the problems that arise when imaging in non-ideal imaging situations using existing iris processing methods found in literature as well as newly developed methods based on general image processing methods. In short, the aim of this report is to answer the two questions: Is the image quality of standard equipment adequate for the purpose? Are there methods for IR robust enough to work under these circumstances?

1.3 Document structure

First, a more in-depth problem description will be presented in chapter 2. Chapter 3 contains an introduction to image analysis and iris recognition concepts to provide with the theoretical background to the methods described in chapter 4. Chapter 5 describes the image databases used, the test system and the tests performed along the results. Finally, chapter 6 discusses the test results, the fulfillment of the goals and presents ideas for further research.

Chapter 2

Problem description

Imaging the iris is restricted due to the anatomical properties of the eye as well as noise introduced in the imaging situation. Eyelids together with eyelashes very often occlude a significant part of the iris, and this problem must be identified and handled in every robust iris recognition method. Also, when imaging eyes under less than perfect conditions, the resolution of the image might be insufficient and artifacts are inevitably introduced in the image as noise and blurring due to poor focus. This chapter will define and describe these problems for which solutions will be described in the methods in chapter 4 and the relative importance will be presented in section 6.1.

2.1 Resolution

The spatial resolution of the image acquired of the iris is of course of great importance for the result of the iris recognition process. Different minimum resolutions have been presented. In [8] Daugman recommends that the iris radius should resolve a minimum of at least 70 pixels in radius and that typical systems use iris images with iris radiiuses of 100 to 140 pixels but does not specify the exact iris image resolution used in his tests. Wildes suggest in [25] a lower radius limit of approximately 64 pixels to adequately discern details in the iris, based on an empirical estimate.

2.2 Occlusion

The eyelids cover the eye to restrict light from entering into the eye when needed. This is a problem for IR when imaging the eye with visible light, as in the case is when using standard cameras. The problem can be solved by illuminating the eye with light outside the visible spectrum and has been done so in commercial applications. However, this thesis is about the application of standard camera equipment which operates in the visible spectrum. Therefore, this biological reaction must be handled.

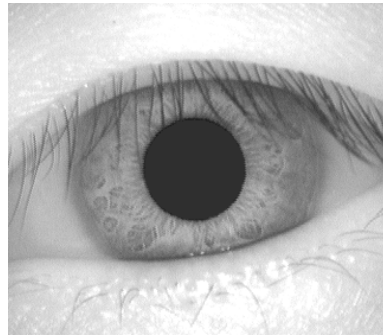


Figure 2.1. Example of occlusion by eyelids and eyelashes from the CASIA database.

Eyelid occlusion causes two problems, one in locating the eye in the image as it destroys the circular shape of the iris in the image and one in the template extraction process as the eyelid can cause a substantial part of the iris pattern to be covered and therefore invalid.

Like the eyelids, eyelashes cause problems in both localization and in the template extraction, but to a lesser extent. Eyelashes are in comparison to the eyelids much harder to identify than eyelids due to their unstructured nature.

2.3 Noise

Iris imaging is a type of measurement and all measurement are subjects to errors which can be modeled and handled as noise. One source of this noise is photon noise, arising as a natural part of light due to the fact that the number of photons hitting an image sensor and generating charge carriers is never exact and can only be described using probability. The noise in the imaging sensors and the surrounding electronics is often modeled as white and additive.

2.4 Reflections

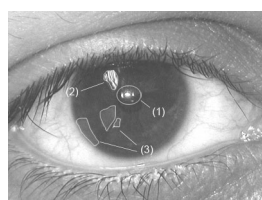


Figure 2.2. Example of reflections: (1) Reflections from the light source (2) Strong reflection from surroundings. (3) Weak reflections

The outermost part of the eye, the cornea, is a transparent layer that protects the eye and from which much of the light is reflected and causing a significant amount of specular reflection. Light sources and surrounding light areas such as windows can be seen projected on the surface of the eye. These reflections cause problems in the IR process, occluding the iris pattern and making the location of the eye harder to determine due to the fact that the reflections distort the annual shape of the eye. Three types of specular reflections can be identified as seen in figure 2.2.

1. High intensity reflections from light sources, causing total occlusion of underlying pattern. Often circular in shape and located inside the pupil boundaries.
2. High intensity reflections from surroundings i.e. windows, causing total occlusion of underlying pattern. Of arbitrary shape.
3. Low intensity reflections from surroundings. Lighting up the underlying pattern, but not causing complete occlusion.

2.5 Compression

When saving the image data to a file, lossy compression is often used. This introduces information loss and can result in artifacts as visible image blocks and a loss of high frequency information in the iris pattern.

2.6 Focus

Many digital imaging systems are restricted to a very limited depth-of-field because of requirements of low demands on lightning and exposure times. In short, imaging under low light and with short exposure times requires a high numerical aperture and this results in a low F-number that limits the depth-of-field. According to Plemmons[19] good focus is obtained in most IR systems through feedback to the user for correct alignment of the eye, which can be a significant obstacle and makes the systems less than fully automatic.

When the eye is imaged outside the depth-of field, the image is blurred and results in poor recognition. If blurred, the iris boundaries become less sharp and results in poor localization, and the high frequency information in the iris pattern is lost which results in poor matching results.

2.7 Light level

When imaging the iris under poor light, the signal to noise ratio decreases and along with image quality and the iris recognition rate decreases. In addition to that, poor light can result in a blurry image due to problems with the auto focus in the camera equipment.

The areas where problems are likely to occur when imaging the iris under non-ideal conditions have now been presented. Methods to resolve the problems will be presented in chapter 4 and the respective importance of these problem areas will be evaluated in chapter 5.

Chapter 3

Theory

This chapter presents the concepts and theory needed for understanding the IR systems and methods presented in this thesis. Where the theory is too voluminous to fit in this thesis an introduction will be presented and pointers given to further reading. First an introduction to biometric identification concepts will be given followed by a presentation of different algorithms used in IR.

3.1 Biometric identification for IR

All biometric identification between two samples of a chosen property of the human anatomy (fingerprints, iris, voice etc) results in a scalar value, indicating how similar the two samples are. For identification of two samples from the same person, this value should indicate great similarity and for samples from different persons this should result in great dissimilarity. For an ideal biometric technology, authentic matches (samples from the same person) would result in a dissimilarity value of zero, indicating that there is no difference between the samples and for impostor matches (samples from different persons) this would result in a dissimilarity value of one, indicating that the samples are completely different.

However, there are no ideal biometric technologies, so dissimilarity values between one and zero will occur in the identification results. An example of this is showed in figure 3.1 which shows the resulting distributions of a set of authentic and impostor dissimilarity values. The distributions overlap, which makes it impossible to separate the two classes completely. Any chosen separation boundary, from now on named s , will give rise to either false rejections (two samples not determined to be from the same person) or false accepts (two samples from two different persons determined to be from the same person).

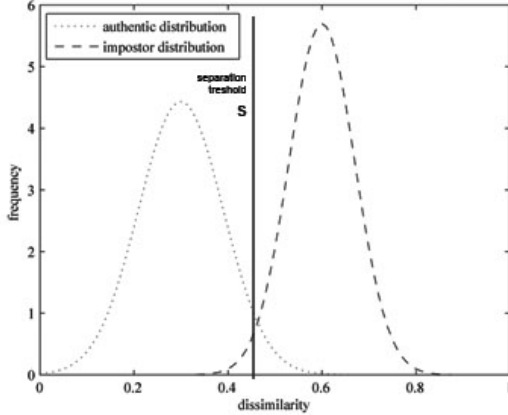


Figure 3.1. Impostor and authentic match result distributions

These errors are measured as FRR, false rejection rate as defined in equation 3.1, and FAR, false acceptance rate as defined in equation 3.2. The equal error rate measure, or ERR, is another performance measure that is defined at the point where FRR and FAR are equal.

$$FRR = \frac{\int_s^1 P_{authentics}(x)dx}{\int_0^1 P_{authentics}(x)dx} \quad (3.1)$$

$$FAR = \frac{\int_0^s P_{impostors}(x)dx}{\int_0^1 P_{impostors}(x)dx} \quad (3.2)$$

Another performance measurement is decidability, d , defined in equation 3.3 which measures the separation of the impostor and authentic distributions and takes in account the mean and standard deviations of the classes. The higher the decidability, the better separation between authentics and impostors and therefore better recognition performance.

$$d = \frac{|\mu_{impostors} - \mu_{authentics}|}{\sqrt{\frac{|\sigma_{impostors}^2 - \sigma_{authentics}^2|}{2}}} \quad (3.3)$$

3.2 Image processing for IR

This section will give an introduction to image processing algorithms and concepts used in IR. This section does not aim to provide for a beginners course to image processing, but rather to explain the methods and algorithms used in this thesis.

3.2.1 Edge detection

Edge detection is a fundamental image analysis technique used for detecting object boundaries and data reduction in an image, see [5], preserving important structures while reducing the amount of data to process significantly. Edge detection is used in IR when locating the iris part of the image, see section 4.2.

Edges in an image are defined as areas with sharp spatial intensity transitions. If looked upon as a continuous 2D function the edges would be the local maximums of the gradient. Assuming this, edge detection is then being reduced to finding max of the derivatives of the image intensity values $I(u, v)$. Unfortunately, a digitized image is not a continuous function but rather a discrete function, so the derivatives must be approximated.

As an image is a 2D signal the approximation of a derivative must be done in a defined direction. To estimate the derivative in any arbitrary direction, two estimates can be done d_u and d_v along the axes of the image and the derivative in the direction ϕ can be calculated according to:

$$d_\phi(u, v) = \cos(\phi) * d_u(u, v) + \sin(\phi) * d_v(u, v) \quad (3.4)$$

The derivatives d_u and d_v are estimated through convolution of the image and derivative filters:

$$\begin{aligned} d_u &= I * h_u \\ d_v &= I * h_v \end{aligned} \quad (3.5)$$

A number of different derivatives filters exist, with different noise reduction and frequency response characteristics. Two common filters: Sobel (see 3.7) and a basic filter pair(see 3.6) are shown below. The Sobel filter [23] is more insensitive to noise, while the basic one is very sensitive to noise but has a higher frequency range.

$$h'_v = h_u = [1 \ 0 \ -1] \quad (3.6)$$

$$h'_v = h_u = \frac{1}{4} \begin{bmatrix} 1 & 0 & -1 \\ 2 & 0 & -2 \\ 1 & 0 & -1 \end{bmatrix} \quad (3.7)$$

Edge detection is used in IR when locating the iris in the image. See section 4.2.

3.2.2 The Canny operator

The Canny operator [3] was designed to be an optimal edge detector, creating a binary edge map from an intensity image in a much more intelligent way than a mere thresholding of an edge strength estimate. The algorithm consist of three steps:

1. Noise reduction through convolution with a Gaussian filter.

2. Estimation of edge strength as described in section 3.2.1, using the Sobel filter pair.
3. Edge tracking is then performed along edges in the image starting in the positions in the image that have an edge strength bigger than a certain threshold (T_1). Tracking is continued, marking only local edge maximums as edges, until the edge strength falls below another threshold, (T_2).

The use of the two thresholds aims to ensure that noisy edges does not break up into fragments and the Gaussian smoothing filter reduces the detectors sensitivity to noise. Increasing the size of the Gaussian filter makes the operator more insensitive to noise but reduces the ability to detect finer edges. The Canny operator is used in [17] and when locating the eyelids using the method described in 4.6.2.

3.2.3 Orientation in an image

Images are two-dimensional signals, and as such, it is sometimes useful to make the assumption that small regions of an image can be locally described as one-dimensional. When this assumption is correct, which it is in the case of natural images except for specific points as corners or line junctions, the local 1D functions describing the image can be estimated through the use of a variety of methods. The local orientation can then be defined as the direction in which the signal can best be described as one-dimensional. For an image only consisting of a white straight line on a black background the local orientation would perpendicular to the line around it and undefined in the surrounding areas. The estimation methods and the underlying theory will not be presented in this thesis, but can be studied in [11].

The orientation of an image can, after being estimated by various methods, be represented as a discrete complex image where the argument of each complex pixel represents the orientation of the corresponding pixel in the original image. The orientation information is used when locating the center of the iris in the method described in section 4.6.1.

3.2.4 The Hough transform

The Hough transform [12], similar to the Radon transform [9], was originally developed in the 1950s for detection of linear traces in bubble chamber photographs, but has been generalized to detect any shape that can be described in a parametric correlation form. The most common use for the generalized Hough transform [2] is the detection of regular curves such as lines, circles and ellipses in images and is very often used together with an edge detection algorithm.

The biggest advantage of the algorithm is that it can find a global description of features in an image such as the circle boundaries of the iris given local measurements. The biggest disadvantages is that it is rather computationally expensive ($O(N^3)$ in the case of circle detection for example) and that it relies on a well done

feature extraction step. The generalized algorithm can be described using these steps:

1. Extract feature points in the image $I(u, v)$, using for example an edge detection algorithm. This results in the feature image $F(u, v)$ which values indicates the presence of a desired feature in that particular position.
2. For all parametric curves $S(\alpha, \beta, \gamma, \dots)$ passing through $F(u, v)$, increase the accumulator $A(\alpha, \beta, \gamma, \dots)$ with $F(u, v)$.
3. Extract N biggest maximums in $A(\alpha, \beta, \gamma, \dots)$ which will correspond to the best fitting curves in the image with corresponding parameters $(\alpha, \beta, \gamma, \dots)$.

The Hough transform is used in IR systems such as [24] and [17] for locating the circular boundaries of the iris. See section 4.2.1 for information on how this method is applied.

Chapter 4

Iris recognition methods

This chapter will describe how iris recognition works, which steps the process consists of and how these steps can be implemented. First, a generalized structure for IR systems will be described, then methods found in literature to implement the different parts of the IR process will be presented followed by a description of methods developed during the course of the thesis work.

4.1 The IR process

A number of iris recognition systems have been studied ([17], [7], [25], [19], [18], [24], [15], [26], [14], [13]) and found to be very similar in structure. The IR pipeline in these systems can be described using these four steps:

1. Image acquisition. Obtaining an image of the subjects eye.
2. Localization and extraction of the iris part in the image.
3. Iris feature extraction. Extraction of discriminating properties of the iris, resulting in a unique iris signature, often called iris template or iris pattern.
4. Matching. Comparison of different templates for degree of match.

All four steps are as important for good recognition, but as the aim of this thesis is not to study the acquisition of eye images this section will focus on steps two to four. These steps can further be divided into the steps shown in figure 4.1 where step two is divided in segmentation and mask generation and step three in normalization and feature extraction. All the steps shown in figure 4.1 will be described in detail under their respective sections together with various implementations of these steps found in literature.

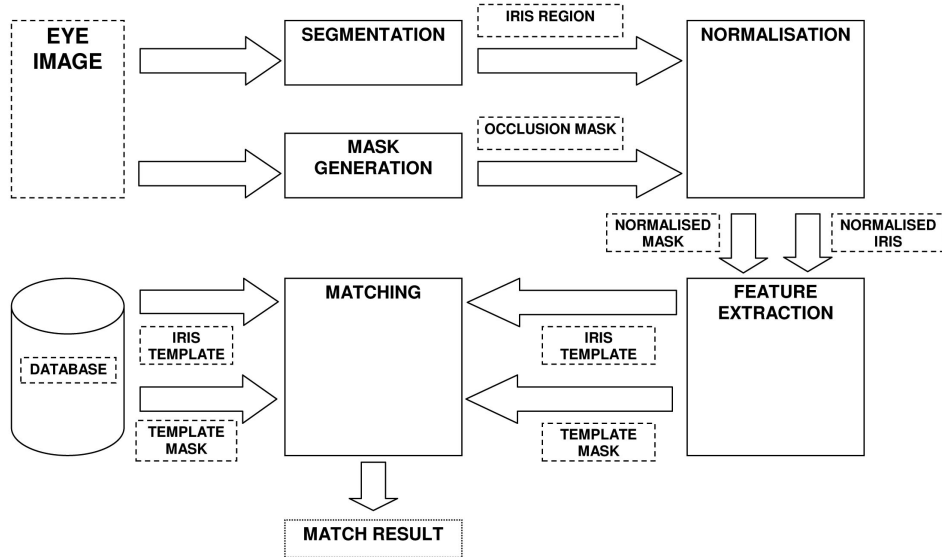


Figure 4.1. Schematic description of a generic IR system.

4.2 Segmentation

The objective of the segmentation step is to locate the iris region in the image. This consists of finding the inner boundary between the pupil and the iris and the outer boundary between the iris and the sclera. These boundaries, although not always perfectly circular, are modeled in most methods as two unconcentric circles, with the exception of the method proposed in [18] in which the boundaries are approximated as ellipses. A result of boundary fitting with a circular model is illustrated in Figure 4.2. Using these models the problem is then reduced to finding the circles or ellipses best describing the iris boundaries. A variety of methods has been proposed to do this and the most successful ones will be presented in this section.

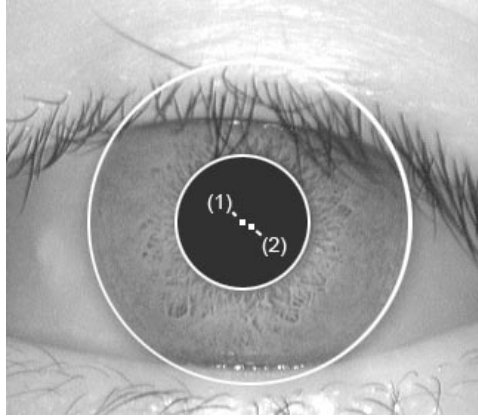


Figure 4.2. Iris segmentation using unconcentric circles.(1) Center of inner circle. (2) Center of outer circle

4.2.1 Hough transform based methods

Methods based on the Hough transform for circles, described in section 3.2.4, have been proposed by Tisse et al. [24], Ma et al.[15] and Wildes et al.[25]. The methods all apply an edge detector to the iris image followed by searching for the best inner and outer circular boundaries for the iris using the Hough transform. The edge detectors used vary between the methods, and in the case of the method proposed in [25] also between detection of the outer and inner boundaries of the iris. These methods all rely on good threshold parameters for the edge detection step, making them sensitive to varying imaging conditions.

4.2.2 Daugmans integro-differential operator

John Daugman presented in 1993 the segmentation method described in [7]. This method is based on his *integrodifferential operator*, defined in equation 4.1 which searches for the best fitting circles for the inner and outer boundaries of the iris. The operator is used twice, once for the inner boundary and once for the outer boundary searching iteratively for the best center coordinates (x_0, y_0) in the image I . This is done by looking for the max value of the derivative in the radius dimension of the result of a circular contour integration. This search is performed iteratively from a coarse scale down to pixel level through convolution with a Gaussian kernel function [21], $G_\sigma(r)$ with decreasing size.

$$\max_{(r, x_0, y_0)} \left| G_\sigma(r) * \frac{\partial}{\partial r} \oint_{r, x_0, y_0} \frac{I(x, y)}{2\pi r} ds \right| \quad (4.1)$$

This operator is frequently referred to in literature and different versions of this operator have been tested, for example in [18] in which a more general model

was applied for the boundaries, modeling the iris as a rotated ellipse rather than a circle.

4.2.3 Methods based on thresholding

Segmentation methods based on the assumption that the iris can be separated from the eye because of the fact that the iris is generally lighter than the pupil and darker than the sclera have been proposed in Cho et al. [4], Zhu et al. [26], and Liam et al. [13]. The iris image is thresholded using an upper and lower intensity limits and then passed on to a circular edge detector. This approach aims to simplify for the edge detection step, which it does, but instead introduces the problem of finding good threshold levels.

4.3 Normalization

After segmentation has been completed, normalization is performed in all studied iris recognition systems to obtain invariance to iris size, position and different degrees of pupil dilation when matching different iris patterns at a later stage. The problem of that the iris can be rotated in the image is not resolved by this transformation, but is instead taken care of during matching.

The method that is widely accepted for doing this is applying Daugmans rubber sheet model [7] to the iris and transforming it into a rectangular block. This transform to polar coordinates is defined in equations 4.2, 4.3, 4.4 and is illustrated in figure 4.3.

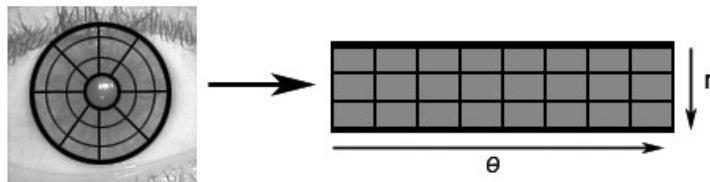


Figure 4.3. Illustration of normalization

$$I(x(r, \theta), y(r, \theta)) \rightarrow I(r, \theta) \quad (4.2)$$

$$x(r, \theta) = (1 - r)x_i(\theta) + r \cdot x_o + \cos(\theta) \cdot (r_i + r \cdot (r_o - r_i)) \quad (4.3)$$

$$y(r, \theta) = (1 - r)y_i(\theta) + r \cdot y_o + \sin(\theta) \cdot (r_i + r \cdot (r_o - r_i)) \quad (4.4)$$

4.4 Mask generation

The problems associated with occlusion (see section 2.2) of the iris by eyelids and eyelashes can be resolved by identifying these areas and marking them as occluded. The occluded areas can be marked as ones in a binary image, or mask, with the same size as the original.

Different methods have been proposed to do this, Daugman [7] used a modified version of his integro-differential operator to detect the eyelids through searching for arcs instead of circles, but does not specify in detail how this is done. Masek [17] proposed to find the eyelids by locating lines by finding the maximum of a linear hough transformation of the image. A own method to do this is presented in section 4.6.2.

4.5 Encoding and matching

The encoding, or feature extraction, aims to extract as many discriminating features as possible from the iris and results in an iris signature, or template, containing these features. The matching process between two templates aims to maximize the probability of a true match for authentic identification tries and minimize false matches for impostors. In other words, images of the same iris taken at different times should be identified as being from the same person and images from different irises should be marked as coming from different persons.

In this section Daugmans methods for encoding and matching [7] will be presented in detail as this method was used in the testing along with an overview of other methods found in literature.

4.5.1 Daugmans method

Since 1993, when Daugman proposed the first successfully tested iris recognition system, many alternate methods have been proposed with the aim of improving recognition rate. However, only a few systems perform as good as Daugmans and none have been as thoroughly tested.

Encoding

Daugman applies a set of Gabor wavelets [6], to extract local phase, $F(r, \theta)$ information utilizing information around the base frequency ω_0 from the normalized iris $I(r, \phi)$ in N discrete positions along the iris according to equation 4.5. The parameters α and β control the size of the wavelet. The resulting 2D phase information is quantized into four levels according to the sign of the imaginary and real part of the result, generating a binary representation, h , of the features. If the feature information in (r_n, θ_n) would be extracted as $(1+i)$ this point ends up in the first quadrant in the imaginary plane and would be encoded as binary (11) and $(1-i)$ would be encoded as binary (10) et cetera. This reduces the amount of information significantly, compressing the feature information to fit into standard magnetic cards.

$$F(r_n, \theta_n) = \int_s \int_{\phi} I(r_n, \theta_n) \cdot e^{-i\omega_0(\theta_n - \phi)} \cdot e^{-(r_n - s)^2/\alpha^2} \cdot e^{-(\theta_n - \phi)^2/\beta^2} d\phi ds \quad (4.5)$$

$$h_{(Re,Im)} = \text{sgn}_{\{Re,Im\}} F(r, \theta) \quad (4.6)$$

Matching

Matching is performed, using the normalized Hamming distance measure defined in equation 4.7, taking into account the occluded regions defined as masks by not comparing the feature points extracted from these regions. The result is the number of bits that are different between the binary codes in the non-occluded regions, divided by the number of bits compared.

$$HD = \frac{\|codeA \otimes codeB \cap maskA \cap maskB\|}{\|maskA \cap maskB\|} \quad (4.7)$$

If the iris images would not be subject to noise and segmentation errors would not occur, the Hamming distance between two pictures taken of the same iris would be 0, however even at the most perfect conditions for imaging this is not the case. Daugman reports that the mean Hamming distance between two iris templates of the same iris, imagined at different occasions and under near perfect conditions, is 0.11 [7].

The theoretical Hamming distance between two different irises results in a Bernoulli trial, or coin toss test, $P_p(m|N)$, where p is the probability that two bits are equal, m is the number of equal bits and N is the total number of bits compared. For uncorrelated iris codes $p = 0.5$. The fractional function associated with the binomial distribution is defined in equation 4.8 where $x = N/m$ is the normalized hamming distance spanning from 0 to 1. Real life examples of these distributions can be seen in figure 5.11.

$$f(x) = \frac{N!}{m!(N-m)!} p^m (1-p)^{(N-m)} \quad (4.8)$$

Invariance of rotation of irises is resolved during matching by performing a series of matchings between rotated versions of the encoded irises and using the best match as the final result.

4.5.2 Other methods

A variety of methods have been purposed in literature and can be roughly categorized into correlation based methods and filter based methods. Correlation based methods utilizes a more direct texture matching approach in comparison to the filter based methods. This section will list a number of successful methods as a pointer to further reading on the subject.

Correlation based methods

Wildes et al. proposed in [25] a method based of normalized correlation of iris patterns, in which the iris images are divided up in laplacian pyramids which are then correlated separately for each individual level, resulting in a matching vector. Fishers linear discriminant [10] is then applied on this vector, resulting in a scalar equality score.

Another method based on correlation, is the one proposed by Miyazawa et. al. in [18]. This method applies band-phase correlation to discriminate between authentic and impostor matches.

Wavelet and filter based methods

To perform a wavelet transform or apply some sort of filter are the most common solutions for feature extraction. A variety of methods and filters have been proposed. Ma et al [15] purposed use of filters similar to [7] together with an enhanced matching method based on an extended version of Fishers linear discriminant. Lim et. al. purposed in [14] a method based on the Haar wavelet transform [22] and a matching algorithm based on a neural network.

4.6 Proposed new methods

Some new methods were developed during the thesis work and are presented in this chapter. The methods were developed when present methods did not perform well enough or to test new approaches that might outperform present solutions.

4.6.1 Segmentation

A new method, based on the idea of first localizing the iris center and then estimating the iris boundaries, was developed. The motivation of this approach is that if the iris center could first be located with good precision in the image, the computational cost would be lower for the segmentation and the result would be less erroneous. The method consists, as mentioned above, of two steps:

1. Estimation of iris center using pattern correlation using the pattern illustrated in figure 4.5.
2. Iris segmentation using the center estimate as an input to a novel method.

These steps will be described further below.

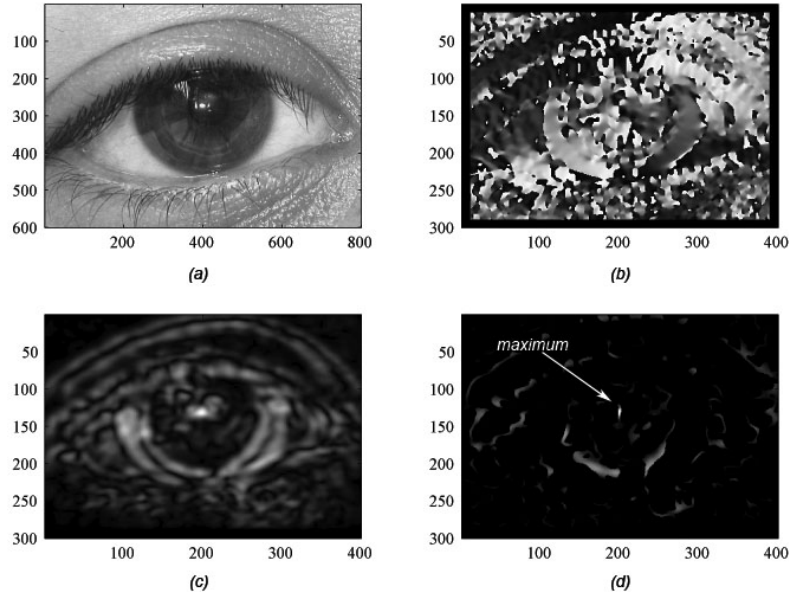


Figure 4.4. Localization steps. (a)Original image, (b) Orientation image $\arg(0)$ is shown, (c) Correlation result, (d) Result after thresholding.

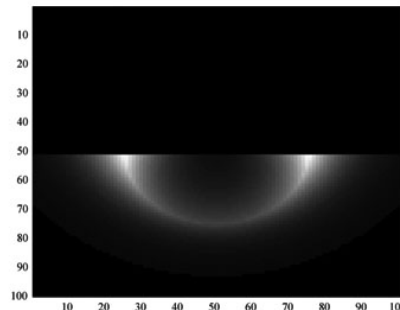


Figure 4.5. Example of localization filter, defined in equation 4.10. $|P|$ is shown.

Iris center estimation

The iris center estimation is done performing the following steps:

1. Down sampling of the iris image to about 15% of the original size, reducing noise and computation time for the later steps.

2. Transformation of image intensity values into a complex valued local orientation map $O(x, y)$, described in section 3.2.3.
3. Correlation, defined in equation 4.9 of an iris orientation pattern P , defined in equation 4.10 with the orientation map.
4. Thresholding of the correlation result, defined in equation 4.11. This thresholding aims to mask out the areas of which the orientation of the image agrees with the orientation of the orientation pattern.
5. Localizing the global maximum of the thresholding result T , indicating the center of the iris (x_0, y_0) .

$$C(u, v) = \int_x \int_y O(x, y) \cdot P(x - u, y - v); \quad (4.9)$$

$$P(x, y) = \begin{cases} e^{-|\sqrt{x^2+y^2}-b_r|/\sigma_b} \cdot e^{-|\frac{y}{y_s}|} \cdot e^{-2i \cdot \tan^{-1}(\frac{y}{x})} & \text{when } y > 0 \\ 0 & \text{when } y < 0 \end{cases} \quad (4.10)$$

$$T(u, v) = \begin{cases} |C(u, v)| & \text{when } |\arg(C(u, v))| \leq \omega_t \\ 0 & \text{when } |\arg(C(u, v))| > \omega_t \end{cases} \quad (4.11)$$

This process is illustrated in figure 4.4 and an example of an iris localization pattern is displayed in figure 4.5.

The idea behind this approach was based upon a lab in the computer vision course "Bildanalys" at the Computer Vision Laboratory, Linköping University. In the lab, blood cells were to be localized using orientation information in the image correlated with a rotation symmetric pattern. This worked in the lab and the idea was to create an optimized filter for locating irises using the same approach. Different iris localization patterns were tested during the development of this method but the pattern defined in 4.10 proved to be the most successful. The filter consists of an orientation part, $e^{-2i \cdot \tan^{-1}(\frac{y}{x})}$ that aims to identify circle-symmetric patterns, multiplied by two weighting functions, one that favors circles with the radius b_r and one favoring orientation information close to the horizontal axis (to avoid errors caused by eyelashes). The filter only matches the lower part of the iris (all values are set to zero for $y < 0$) to avoid localization errors when the iris is occluded by the top eyelid. This restriction made the method more robust to noise and provided for better accuracy.

Boundary detection

The next step of the proposed method is the actual boundary fitting of the iris. This is done in four steps:

1. Polar transform of pixels around the located iris center. (equation 4.12).

2. Edge detection through derivation along the radius axis (equation 4.13).
3. Integration of the result along the theta dimension, normalizing the result with the maximum edge value in the theta dimension and the circumference (equation 4.14). This is done ignoring the information in the theta span from $\frac{\pi}{4}$ to $\frac{3\pi}{4}$. This slice is skipped to avoid errors in the edge map caused by eyelashes and eyelids.
4. Search for the best circle boundary with the center coordinates (x_0, y_0) and circle radius r . (equation 4.15)

$$P(x_0, y_0, r, \theta) = I(x_0 + r \cdot \cos(\theta), y_0 + r \cdot \sin(\theta)) \quad (4.12)$$

$$E(x_0, y_0, r, \theta) = \frac{\partial}{\partial r} P(x_0, y_0, r, \theta) \quad (4.13)$$

$$E_{sum}(x_0, y_0, r) = \frac{\int_{-\frac{\pi}{4}}^{\frac{5\pi}{4}} E(x_0, y_0, r, \theta)}{\max_\theta [E(x_0, y_0, r, \theta)] \cdot 2\pi \cdot r + \gamma} \quad (4.14)$$

$$\max_{\{r, x_0, y_0\}} [E_{sum}(x_0, y_0, r)] \quad (4.15)$$

This method is similar to Daugmans in section 4.2.2, with the improvement of the normalization in step three and ignoring the upper, often occluded, part of the boundaries when fitting the circles creating a more noise-robust operator.

4.6.2 Mask generation

A new method was developed, using a new approach. The development of this method was motivated by the poor results of the method found in Libor Masek's open source method, when applied on noisy images. An easily implemented method was developed to provide for automated masking. The method can be described in three steps:

1. Edge detection of the image, using the Canny operator (see section 3.2.2)
2. Localization of eyelid edges, one by one using a new operator, performing summation along probable eyelid edges. See figure 4.7.
3. Creation of a binary map, indicating the regions above and under the top and bottom eyelids respectively as occluded.

The new operator is defined in equation 4.16. The operator uses a summation map, M defined in equation 4.17 and shown in figure 4.7, which defines the curves along which the edges are summed up. This function was developed to describe the curvature of the eyelids. The constant c_{form} is a form factor for the operator, determining the shape. A value of 0.8 for c_{form} proved to work very well. The operator is applied with its center placed in the pupil center (x_0, y_0) .

$$E_{sum}(d) = \sum_x \sum_y \begin{cases} I(x - x_0, y - y_0) & \text{when } M(x, y) = d \\ 0 & \text{when } M(x, y) \neq d \end{cases} \quad (4.16)$$

$$M(x, y) = \sqrt{x^2 + \left(\frac{y}{c_{form}}\right)^2} \cdot |y| \quad (4.17)$$

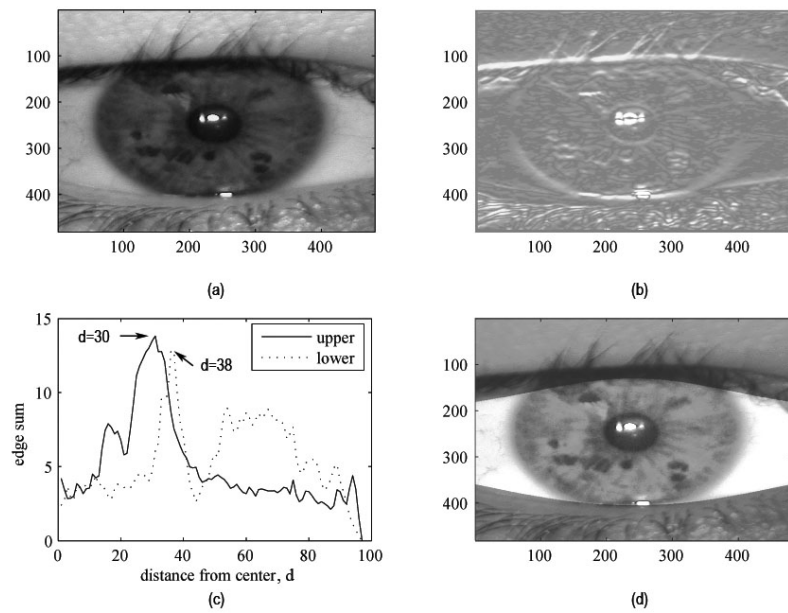


Figure 4.6. Illustration of masking. (a) Eye image. (b) After edge detection. (c) Edge sums. (d) Result, mask marked as shaded areas.

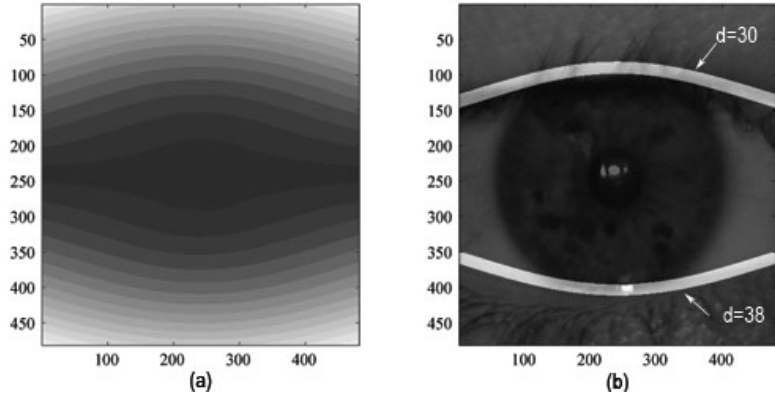


Figure 4.7. (a) Summation map, M. (b) Eyelid localization result with located contours.

The method is similar to the generalized Hough transform, see section 3.2.4 but with a more restricted parameter space. Only one parameter, d , is used for describing the eyelid arcs, in comparison to Maseks method [17] which describes the eyelids with lines which requiring a two-dimensional parameter space. Other methods require even more parameters, making the methods computationally very expensive.

Chapter 5

Evaluation

This chapter will present how the evaluation of methods and images was done, a description of the images tested, how the test system was constructed and finally a description of the tests performed and their results. The aim of the evaluation was to test the respective influence of the problem areas presented in chapter 2, the performance of the methods in chapter 4 on an image database consisting of images from a standard camera.

5.1 The IrisLAB test system

IrisLAB is our system developed in MATLAB for the testing of iris recognition methods and iris images during the course of the thesis work. The system was designed to provide for an efficient environment for testing images and methods for IR.

The system is in part based upon an open source MATLAB system, IrisCode, developed by Libor Masek for his thesis [17], generalized and extended with a database connection, result presentation and more methods for segmentation and mask generation. To base the system on open source code enabled a much more rapid development process, freeing time to improve methods and perform more tests instead of just implementing methods described in literature. The extension of the open source system was focused on the segmentation part as that was the area that performed too poor for the class of images tested. The matching and encoding was considered to work well enough, but the presentation of the results was improved and the need for running large, well specified, tests was resolved.

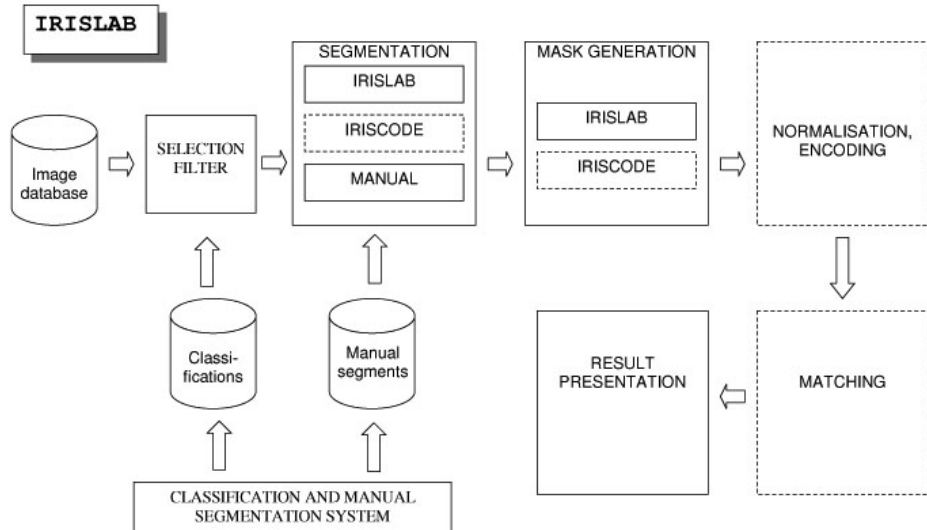


Figure 5.1. IrisLAB overview, dashed parts were incorporated from Libor Maseks open source system.

To perform a test using the system, the test case is specified in a configuration file, containing a structure specifying all parameters for the test, i.e. dataset to test and which methods (i.e. IrisLAB or IrisCode methods for segmentation and mask generation) to use along with their parameters. The images to perform tests on are specified using a SQL query, returning a list of image numbers for the system to load. This solution enables the use of classification data (i.e. light level) when selecting images for testing. The images are loaded and then passed on to be segmented by a specified segmentation method. If manual segmentation is specified, the manual segmentation information from the database is used. Occluded pixels are then marked using a masking method, and passed on to normalization and encoding using Daugmans methods and Maseks MatLAB implementation. Matching is finally performed and the result is presented. See figure 5.2 for a screen shot of the system.

The classification and manual segmentation data is generated using Eye View, a new MATLAB tool developed for the purpose. The user interface of this tool is presented in figure 5.3. In Eye View an iris image can be manually segmented (both iris and eyelid boundaries) and categorized according to light level, level of focus and amount of reflections present, grading each property in three levels.

IrisLAB was developed for MATLAB R14, using MySQL 5.0 for the database.

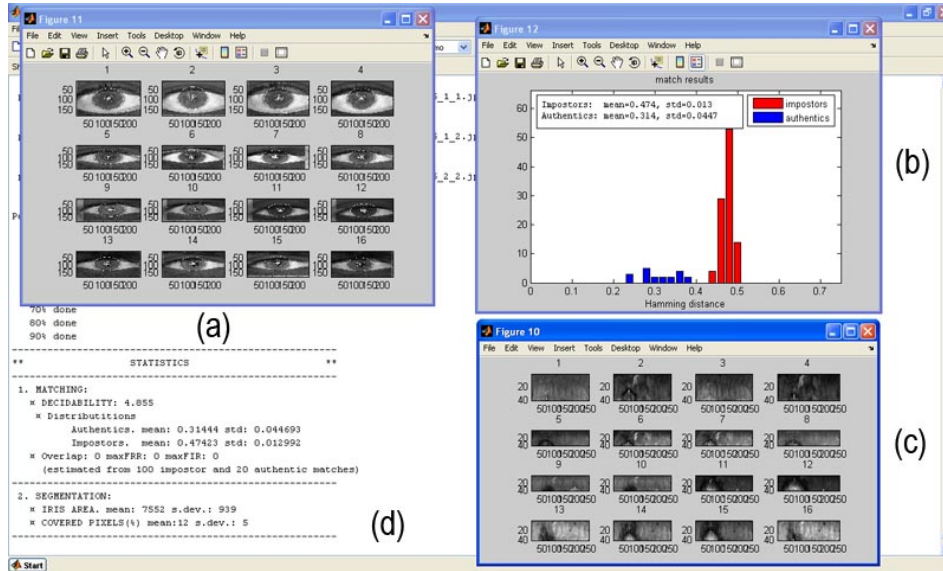


Figure 5.2. Screenshot of IrisLAB. (a) Segmentation and mask results. (b) Match result (c) Normalization result. (d) MATLAB command window displaying statistics.

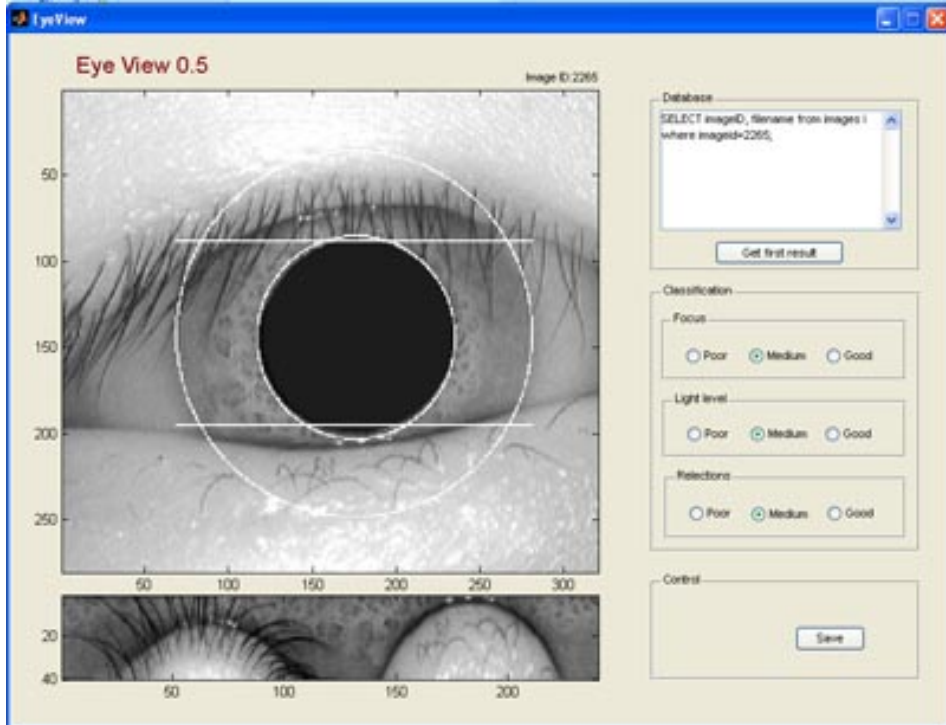


Figure 5.3. Screenshot of Eye View.

5.2 Iris image databases used

To test the performance of IR on standard cameras, a database of images from this equipment had to be obtained. At first, several sessions of imaging with different types of cameras available was considered but disregarded when large public iris databases were found. This freed a substantial amount of time for test and development, which would otherwise had been spent imaging and organizing photo sessions. Two public databases were chosen to perform tests upon: the UBIRIS database and the CASIA database, the former was chosen for utilizing standard equipment and the latter was chosen to provide for a comparison. The databases will be described further below.

5.2.1 The UBIRIS database

The UBIRIS database [20] was collected by Hugo Proenca and Luis A. Alexandre of Universidade da Beira Interior, Portugal, to provide for a noisy database for the use of development of robust IR algorithms. The camera equipment used was a 4 mega pixel Nikon E5700 and can be considered to represent standard imaging equipment. The database is composed of 1877 images collected from 241 persons.

Images in the database were captured in two sessions: the first aiming to minimize noise factors and the second to simulate a noisy environment with minimal collaboration from the subjects. Proenca and Alexandre categorized the images according to image quality as described in [20] but did not make this information available to the public. Thus, to enable a comparison between different types of noise and noise levels the images had to be manually classified. This was done using Eye View, see section 5.1, the tool developed for this purpose.

5.2.2 The CASIA database

The CASIA database [1] was collected by Institute of Automation, Chinese Academy of Sciences and provides with a high resolution, almost noise free, database. This database is often used in literature to compare different IR methods. In this thesis it is used to provide for a comparison of the segmentation methods. The version 1.0 of the database was used and consists of 756 iris images from 108 eyes.

5.3 Tests

This section presents the tests performed and their results. The aim of the tests was to measure the respective influence of the problem areas concerning image quality (tests 5.3.2 to 5.3.8), performance of segmentation and masking methods (tests 5.3.9 and 5.3.10) and finally an overall performance test (test 5.3.11 to evaluate the matching performance using the UBIRIS database).

5.3.1 Encoding parameters

Before measuring the accuracy of recognition under different circumstances, the parameters used for normalization and for the Daugman encoding method, see section 4.5.1, had to be determined.

As for the the UBIRIS database, the parameters for encoding were determined experimentally using a subset of the UBIRIS database, optimizing for intra session matching. The images were first down sampled by a factor of 50% to speed up the processing and then normalized to a size of 500x40. The template size was fit to match actual iris resolution in the image, based on an manual estimate. Various parameters were tested and the set of parameters generating the best decidability were chosen. The parameters are presented below, see table A.1 for complete list of test results.

For the CASIA image database the optimum parameters for encoding were acquired from Libor Maseks thesis [17]. and are presented in table 5.1 to enable a comparison with the UBIRIS parameters.

Database	Normalized size	Number of filter sets	$\sigma \cdot \lambda$	λ_1	λ_2
CASIA1	240x20	2	0.5	11	22
UBIRIS	500x40	1	0.6	20	-

Table 5.1. Optimum parameters for image databases

In Maseks implementation of Daugmans encoding method, the information in the radius dimension is not used, setting the α constant in equation 4.5 to infinity and utilizing a constant, using $\sigma \cdot \lambda$ as β . Note that the base wavelengths, in pixels, are presented in table 5.1 and not the base frequencies.

For the CASIA database, two base wave lengths was found to be optimal (λ_1 and λ_2), while the UBIRIS database was optimally encoded using only one. The results are similar, both parameter sets utilizing texture information in the mid frequency range.

5.3.2 Resolution

The aim of this test was to measure the importance of spatial resolution for IR. Images were down sampled to various resolutions using bi cubic interpolation, normalized to a template size of 500x40, encoded with the optimum parameters described in 5.3.1 and then matched using 4 rotational shifts in both directions (± 3 degrees). Images classed as poor quality (light level poor and cover degree less than 30 percent) were excluded from the data sets. All images tested were manually segmented to exclude segmentation errors in the result. Three different data sets were used:

- DS1: The first data set that was used contained 50 pictures from the UBIRIS dataset, half from the first session and half from the second session, producing 1175 impostor and 50 authentic match results.
- DS2: The second data set that was used contained 45 pictures from the UBIRIS dataset from the first session, producing 969 impostor and 21 authentic matches.
- DS3: The third data set that was used contained 35 pictures from the UBIRIS dataset from the second session, producing 576 impostor and 19 authentic matches.

The results are presented in figure 5.4 and 5.5. The jagged look of the curves in figure 5.4 is most probable due to the down sampling errors and because of the limited data sets used. The three data sets follow the same trend, the decidability dropping and false rejections climbing at a scale of 0.25 indicating a minimal iris outer radius of about 45 pixels.

5.3.3 Noise

The aim of this test was to measure the reduction of recognition level when additive noise is added to the picture, simulating a poor image sensor. Images were sampled

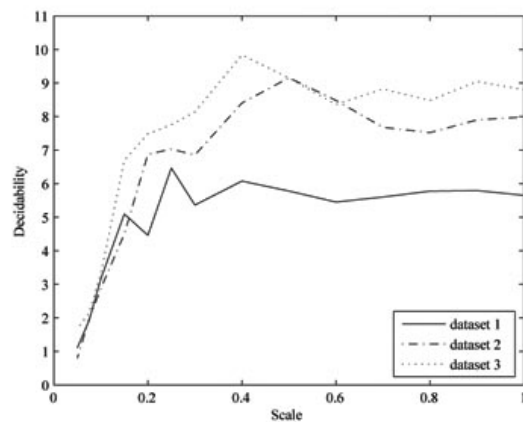


Figure 5.4. Resolution test: scale vs decidability

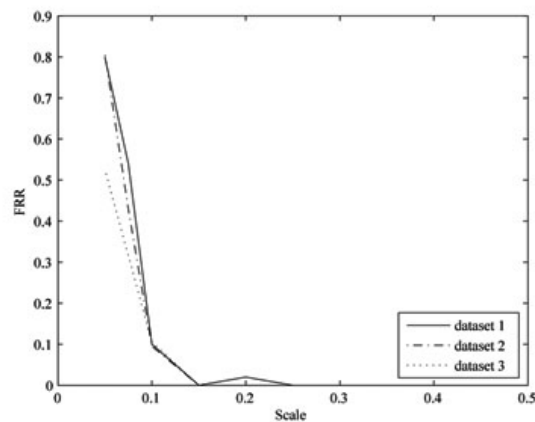


Figure 5.5. Resolution test: scale vs FRR when FAR=0

down by 50 percent to remove most of the noise already present in the image and then gaussian white noise was added. Two test sets were used, DS1 and DS2, identical to the sets used in the resolution test. Encoding parameters and template size was also identical to the resolution test.

The aim of the test on DS1 was to measure the over all performance for both inter and intra session matching. The aim of the test on DS2 was to compare the results of the results of the first dataset to a dataset that had a better quality , as images from session one contained less specular reflections.

The results are presented in figure 5.6 and 5.7. The decidability and false rejection rate indicates no loss in recognition for a SNR bigger than about 30 but dropping for SNRs below that. As a comparison, VHS video has a SNR of about 38 and 30 is considered a lower limit on video signals. This test shows that no extraordinary demands on noise level is necessary.

5.3.4 Reflection

The aim of this test was to measure the reduction of recognition level when reflections are present in images of the iris. The UBIRIS database was used, with images from both sessions and the images were sorted into three reflection classes as described in section 5.2.1. The test sets used were from images in the database were classified as poor, ok and good reflection level respectively or were from the same person having an image in the tested class with a lower level of reflections. Images classified as having a poor light level and a eyelid cover degree of 50 percent or more were excluded from the test sets. Results are presented in table 5.2.

Reflection level	Decidability	Authentic matches	Impostor matches
Poor	4.79	25	146
Ok	6.44	37	1188
Good	6.60	29	1196

Table 5.2. Reflection level test results. All three test had FRR=0 and FAR=0

The results indicate that reflections are not a big error source in recognition, even when the amount of reflections present is rather big the decidability does not drop significantly.

5.3.5 Occlusion

The aim of this test was to measure the effect of eyelid occlusion on recognition. Images classified as having a focus level of better than poor to provide for a homogeneous data set with good recognition performance. These images were tested with occluded pixels marked as invalid, resulting in decidability values d_1 and without marking any invalid pixels, resulting in decidability values d_2 . The results are presented in table 5.3.

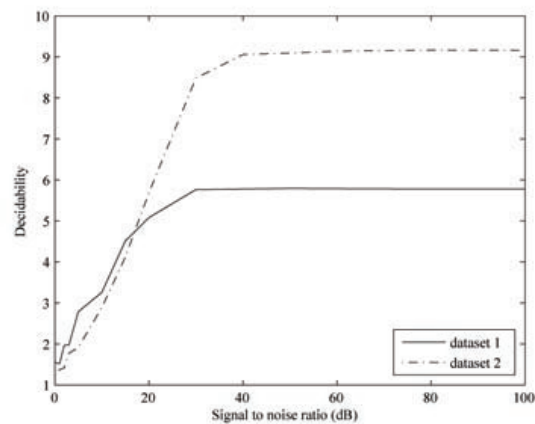


Figure 5.6. Noise test: SNR vs decidabilty

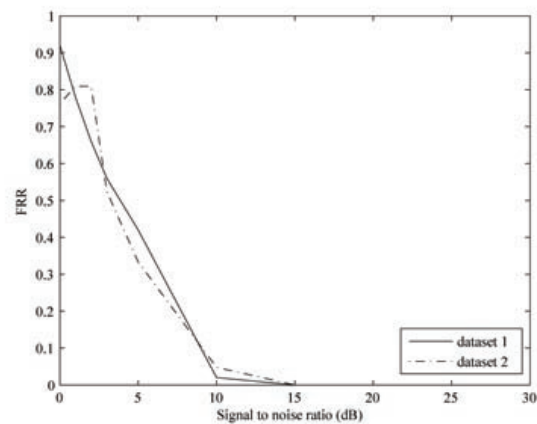


Figure 5.7. Noise test: SNR vs FRR when FAR=0

Occlusion (%)	d_1	d_2	Authentic matches	Impostor matches
6	5.4889	4.9809	37	824
18	4.8603	4.1806	27	1198
35	3.2094	3.2182	5	86

Table 5.3. Occlusion level test results. All three test had FRR=0 and FAR=0

The results indicate that even if a significant area of the eye is covered recognition is still possible, but with lower performance. Also, when comparing the use of a mask, not using the occluded regions when matching, with not using a mask the difference in decidability is small, indicating that a masking of occluded pixels is not vital.

5.3.6 Focus

The aim of this test was to measure the reduction of recognition level when the level of focus decreases in images of the iris. The UBIRIS database was used, with images from both sessions and the images were sorted into three focus classes as described in section 5.2.1. The test sets consisted of images in the database classified as having poor, ok and good focus level or being from the same person having an image in the tested class with a better level of focus. Images classified as having a poor level of reflections and a eyelid cover degree of 50 percent or more were excluded from the test sets. Results are presented in table 5.4.

Focus level	Decidability	Authentic matches	Impostor matches
Poor	4.62	51	939
Ok	5.38	42	1183
Good	9.18	15	615

Table 5.4. Focus level test results. FRR/FAR at poor level 0.0058824/0.0063898.

The test result indicate that good focus is important to achieve excellent matching results, but for lower levels of focus matching works, indicating that perfect focus is not vital. The image information used in the encoding resides in the mid frequency range, which may explain why the blurring and thus the loss of the high frequency components does not affect the matching performance more than this.

5.3.7 Light

The aim of this test was to measure the reduction of recognition level at different light levels in images of the iris. The UBIRIS database was used, with images from both sessions and the images were sorted into three light level classes as described in section 5.2.1. The test sets used were from images in the database classified as having poor, ok and good light level respectively or were from the same person

having an image in the tested class with a better level of light. Images classified as having a poor reflection level and a eyelid cover degree of 50 percent or more were excluded from the test sets. Results are presented in table 5.5.

Light level	Decidability	Authentic matches	Impostor matches
Poor	3.71	34	822
Ok	6.32	41	1188
Good	10.24	20	415

Table 5.5. Light level test results. FRR/FAR at poor level = 0.0256/0.00122

This test shows that light level is very important, as the decidability drops quickly with the light level in the image. It could also be seen in the images that the level of focus dropped with the light level, indicating that the camera had trouble focusing when imaging with little light.

5.3.8 Compression

The aim of this test was to measure the reduction of recognition level when the images are subjects to JPEG compression. The test set used was the first of the test sets defined for the resolution tests. Encoding parameters and template size was also identical to the resolution test. Images were sampled down by 50 percent to remove most of the noise and then compressed to different levels of quality and saved as a JPEG file using a built in MATLAB function.

The results are presented in figures 5.8, 5.9, and 5.10. This test shows that a surprisingly high level of compression can be performed on the images without a loss of recognition. Reducing the image file size to as much as 10% of the original size did in this test not affect the matching performance.

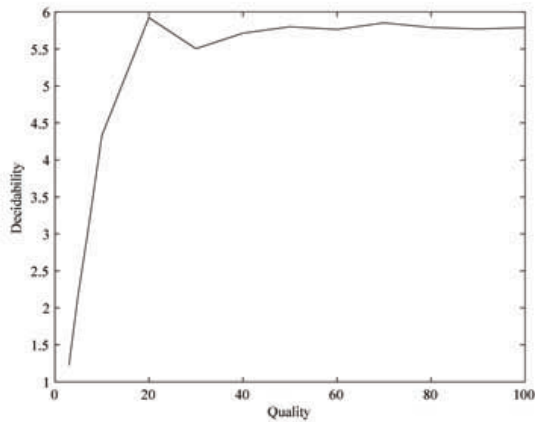


Figure 5.8. Compression test: Quality setting vs decidability

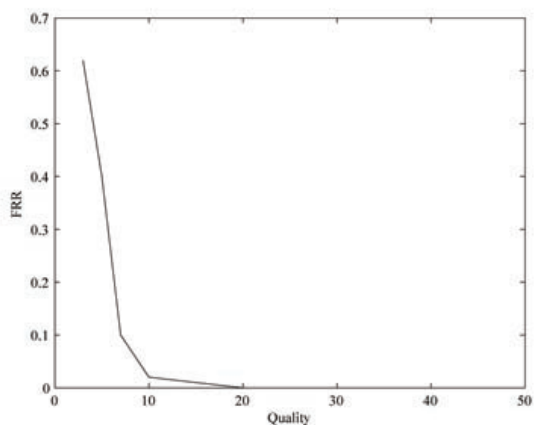
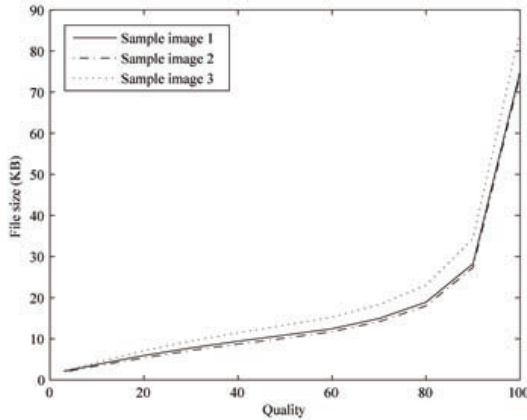


Figure 5.9. Compression test: Quality setting vs FRR when FAR=0

**Figure 5.10.** Compression test: Quality setting vs file size

5.3.9 Segmentation methods

Segmentation performance was evaluated on the UBIRIS image database by applying the Irislab method, described in 4.6.1 and the Iriscode method developed by Libor Masek [17]. A total number of 224 iris images were divided up in four categories according to session and level of occlusion. Low occlusion corresponds to a level of occlusion of less than 25% and high occlusion level corresponds to a level of more than 25%. Among the images in the database, some were sorted out from the test results and marked as bad images, indicating that a correct segmentation would be impossible. These images include fully occluded irises by the eyelids and images with so poor focus that the boundaries of the iris could not be determined by visual inspection.

The results are presented in table 5.6.

Session	Occlusion	Method	Images	Errors	Bad images
1	Low	Irislab	52	0	0
	Low	Iriscode	52	9	0
1	High	Irislab	53	2	5
	High	Iriscode	53	15	5
2	Low	Irislab	69	1	14
	Low	Iriscode	69	24	14
2	High	Irislab	50	8	15
	High	Iriscode	50	26	15
Both	All	Irislab	224	11	34
Both	All	Iriscode	224	74	34

Table 5.6. Segmentation results

Both methods, as expected, had lower performance when the occlusion degree was higher. This was expected as less of the iris boundaries was visible in the image due to the occlusion. Images from session one proved easier to segment for both methods, due to the fact that these images have a generally higher quality.

The overall performance of the IrisLAB method, only failing in 5% of the test-cases, proved to be significantly better than the IrisCode method with failures in 33% of the testcases. It must be added though, that in [20] an evaluation of Maseks method on the UBIRIS database resulted in an error rate of about 15% depending on the parameters chosen. The difference is probably due to the chosen parameters, use of a different subset of the database or differences in the implementation of the method.

In [20] Proen  a and Alexandre also presents the performance of Maseks method on the CASIA database. Their tests resulted in an error rate of about 17%, again depending on the parameters chosen. As a comparasion the IrisLAB method was also tested on this database, resulting in a near-perfect segmentation error rate of 2% when testing a sample set of 200 images.

The over all performance of both methods evaluated proves that images from a standard camera can be segmented an thus used for IR with reasonable performance.

5.3.10 Mask methods

To evaluate the accuracy of mask generation on the UBIRIS database, two methods were tested: Maseks IrisCode method based on the linear Hough transform and the IrisLAB method presented in section 4.4. Maseks IrisCode method proved to be rather unsuccessful on the UBIRIS database. After an initial parameter optimization only about 10% of the generated masks were correct and the method was discarded. The IrisLAB method was tested on 100 random images from both sessions of the UBIRIS database resulting in 3% bad masks, proving the method to be successful on this dataset.

5.3.11 Recognition performance

To evaluate the recognition performance of iris images from standard cameras, images from the UBIRIS database were used. Two test sets were assembled, using images from both sessions:

- DS4: This dataset contained images with no restrictions on quality, resulting in 300 authentic and 19900 impostor match results from both sessions. This dataset was assembled to provide for a random sample of the database.
- DS5: This dataset contained a subset of images of DS4, excluding pictures with poor focus and those having an iris cover degree of more than 40%. This dataset resulted in 99 authentic and 5466 impostor match results. This dataset was assembled to simulate imaging under slightly better conditions.

The images were manually segmented to exclude effects of segmentation errors. The results of this test is presented in figures 5.11 and 5.12. For DS4 a threshold

could not be chosen to perfectly separate the impostor from the authentic matches resulting in an equal error rate of 10%. To allow for no false acceptance matches, 25% of the images would be falsely rejected. For DS5, the authentics and the impostor matches did not overlap at all, resulting in perfect recognition. This test indicates that standard equipment can be used in an IR system even though, as in the case of DS4, 25% would be falsely rejected, this could easily be resolved by taking multiple images of the same eye.

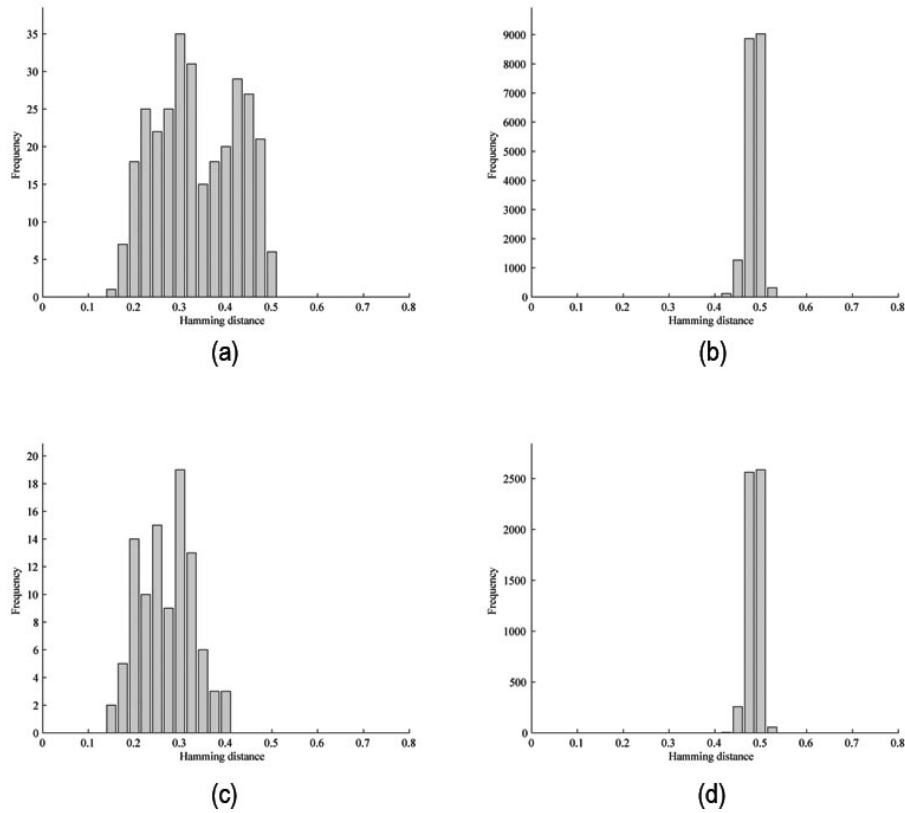


Figure 5.11. Distributions (a) DS4 Authentics, (b) DS4 Impostors, (c) DS5 Authentics, (d) DS5 Impostors

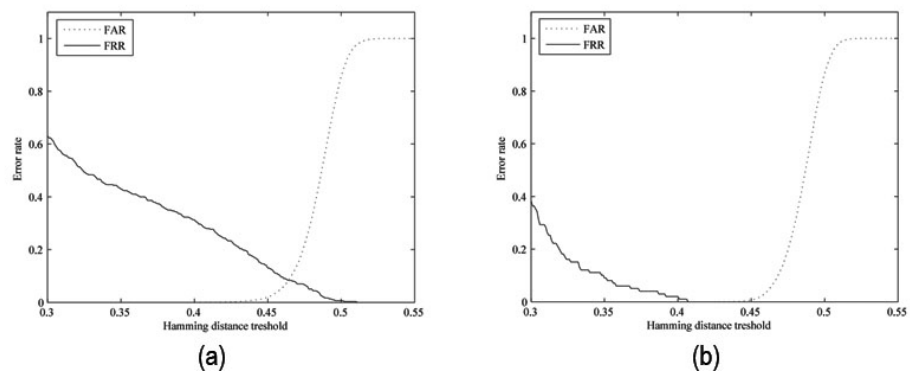


Figure 5.12. Error rates (a) DS4 (b) DS5

Chapter 6

Discussion

In this chapter the results from the evaluation in the previous chapter will be discussed and their implications on the result. The fulfillment of the aim of this thesis and what could have been done better will be discussed. In addition ideas for future work will be presented.

6.1 Summary of results

By using the test results from chapter 5 it can be concluded that an IR system can be constructed using standard camera equipment, and the performance of such a system would be depending on the quality of the images obtained. Concerning the image quality, the light level proved to be the most important image quality factor followed by focus, reflections and level of occlusion. An iris radius of 45 pixels was found to be necessary for good recognition performance. It was also found that images could be compressed to 10% of their original size without affecting the recognition rate. Methods found in literature were not sufficient to provide for a working IR system using images from standard equipment, but new methods were developed to show that such a system could be constructed.

6.2 Fulfillment of goals

As far as the presented goals are concerned they are fulfilled. Image quality from standard cameras has been found to be sufficient for IR purposes and robust methods have been found or developed. Only one matching method was evaluated and the exact safety of a IR system based on standard equipment was not assessed, but neither finding the optimal matching method or the performance of an actual system was the goal of this thesis.

6.3 Future work

This thesis has shown that an IR system can be constructed using standard camera equipment and presents methods that works under these circumstances. The real life performance of such a system was not assessed as that would have required the construction and evaluation of the actual iris imaging that is not discussed in this thesis. To construct such a system would be an interesting project indeed and would give rise to new problems and interesting solutions. If such a project give a fruitful result, IR recognition could soon be much more common than it is today. It would also be interesting to investigate the use of more encoding and matching methods to perhaps improve recognition rate. A system for automatic assessment of image quality and image device control to improve the imaging is another interesting project.

Bibliography

- [1] Casia iris image database. <http://www.sinobiometrics.com>.
- [2] D. H. Ballard. Generalizing the hough transform to detect arbitrary shapes. In *Pattern Recognition*, volume 13, pages 111–122, 1981.
- [3] J. Canny. A computational approach to edge detection. *IEEE Transactions on Pattern Analysis and Machine Intelligence*, 8:679–698, November 1986.
- [4] Dal Ho Cho, Kang Ryoung Park, and Dae Woong Rhee. Real-time iris localization for iris recognition in cellular phone. In *SNPD*, pages 254–259, 2005.
- [5] P. E. Danielsson. *Kompendium i Bildanalys*. Linköping, 2005.
- [6] J.G. Daugman. Uncertainty relation for resolution in space, spatial frequency and orientation optimized by two-dimensional visual cortical filters. *J. Opt. Soc. Am.*, 2(7):1160–1169, 1985.
- [7] John G. Daugman. High confidence visual recognition of persons for a test of statistical independence. *IEEE transactions of pattern analysis and machine intelligence*, 15:1148–1161, November 1993.
- [8] John G. Daugman. How iris recognition works. In *Proceed. of 2002 Intern. Confer. on Image Processing*, volume 1, 2002.
- [9] Stanley R. Deans. *The Radon Transform and Some of Its Applications*. John Wiley & Sons, New York, 1983.
- [10] R. A. Fisher. The use of multiple measurements in taxonomic problems. *Annals of Eugenics*, 7:179–188, 1936.
- [11] G. H. Granlund and H. Knutsson. *Signal Processing for Computer Vision*. Kluwer Academic Publishers, 1995. ISBN 0-7923-9530-1.
- [12] P V C Hough. Method and means for recognizing complex patterns. u. s. patent 3,069,654, 1962.
- [13] Lye Liam, Ali Chekima, Liau Fan, and Jamal Dargham. Iris recognition using self-organizing neural network. *IEEE, 2002 Student Conference on Research and Developing Systems*, pages 169–172, 2002.

- [14] S. Lim, K. Lee, O. Byeon, and Kim T. Efficient iris recognition through improvement of feature vector and classifier. *ETRI Journal*, 23(2):61–70, 2001.
- [15] Li Ma, Tieniu Tan, Yunhong Wang, and Dexin Zhang. Local intensity variation analysis for iris recognition. *Pattern Recognition*, 37(6):1287–1298, 2004.
- [16] T. Mansfield, G. Kelly, D. Chandler, and J. Kane. Biometric product testing final report, March 2001. This is an electronic document. Retrieved: July 2, 2006 from <http://www.cesg.gov.uk/site/ast/biometrics/media/BiometricTestReportpt1.pdf>.
- [17] Libor Masek. Recognition of human iris patterns for biometric identification., 2003. This is an electronic document. Retrieved: February 12, 2006 from <http://www.csse.uwa.edu.au/~pk/studentprojects/libor/>.
- [18] K. Miyazawa, K. Ito, T. Aoki, K. Kobayashi, and H. Nakajima. A phase-based iris recognition algorithm. In *ICB06*, pages 356–365, 2006.
- [19] R. Plemons and M. Horvath et. al. Computational imaging systems for iris recognition. In *Proceed. of SPIE 5559*, pages 346–357, 2004.
- [20] Hugo Proen  a and Lu  s A. Alexandre. Ubiris: A noisy iris image database. In *Proceed. of ICIAP 2005 - Intern. Confer. on Image Analysis and Processing*, volume 1, pages 970–977, 2005.
- [21] Wikipedia The free encyclopedia. Gaussian blur. This is an electronic document. Retrieved: August 1, 2006 from http://en.wikipedia.org/wiki/Gaussian_blur.
- [22] Wikipedia The free encyclopedia. Haar wavelet. This is an electronic document. Retrieved: August 1, 2006 from http://en.wikipedia.org/wiki/Haar_wavelet.
- [23] Wikipedia The free encyclopedia. Sobel. This is an electronic document. Retrieved: August 1, 2006 from <http://en.wikipedia.org/wiki/Sobel>.
- [24] C. Tisse, L. Martin, L. Torres, and M. Robert. Person identification technique using human iris recognition, 2002.
- [25] R.P. Wildes, J.C. Asmuth, G.L. Green, S.C. Hsu, R.J. Kolczynski, J.R. Matey, and S.E. McBride. A system for automated iris recognition. In *WACV94*, pages 121–128, 1994.
- [26] Y. Zhu, T. Tan, and Y. Wang. Biometric personal identification based on iris patterns. In *ICPR00*, pages Vol II: 801–804, 2000.

Appendix A

Full test results

A.0.1 UBIRIS Encoding parameters

A.0.2 Full resolution test results

Number of scales	$\sigma \cdot \lambda$	λ_1	λ_2	λ_3	Decidability
1	0.5	50	-	-	4.0564
1	0.5	40	-	-	4.5029
1	0.5	35	-	-	4.7250
1	0.5	30	-	-	4.8870
1	0.5	27	-	-	5.0501
1	0.5	25	-	-	5.1288
1	0.5	22	-	-	5.2137
1	0.5	21	-	-	5.2389
1	0.5	20	-	-	5.2274
1	0.5	19	-	-	5.2490
1	0.5	18	-	-	5.2136
1	0.5	15	-	-	5.1240
1	0.5	10	-	-	4.3069
1	0.5	5	-	-	2.5223
1	0.8	19	-	-	4.7359
1	0.7	19	-	-	5.0671
1	0.6	19	-	-	5.3385
1	0.55	19	-	-	5.3624
1	0.5	19	-	-	5.2490
1	0.4	19	-	-	5.0136
1	0.3	19	-	-	4.6890
1	0.8	20	-	-	4.8834
1	0.7	20	-	-	5.2096
1	0.6	20	-	-	5.4031
1	0.55	20	-	-	5.3768
1	0.5	20	-	-	5.2274
1	0.4	20	-	-	5.0083
1	0.3	20	-	-	4.6634
2	0.8	15	30	-	4.7575
2	0.7	15	30	-	5.2280
2	0.6	15	30	-	5.2049
2	0.5	15	30	-	5.0950
2	0.4	15	30	-	4.9000
2	0.3	15	30	-	4.5320
2	0.8	20	40	-	4.6609
2	0.7	20	40	-	4.8790
2	0.6	20	40	-	4.9327
2	0.5	20	40	-	4.8827
2	0.4	20	40	-	4.6358
2	0.3	20	40	-	4.2558
3	0.6	15	30	60	4.1939
3	0.5	15	30	60	4.5617
3	0.4	15	30	60	4.0826

Table A.1. Test results for parameter optimization for UBIRIS database.

Scale	Decidability	FRR	FAR
1	5.6502	0	0
0.9	5.794	0	0
0.8	5.7771	0	0
0.7	5.6033	0	0
0.6	5.4501	0	0
0.5	5.7802	0	0
0.4	6.0749	0	0
0.3	5.3615	0	0
0.25	6.4642	0	0
0.2	4.4592	0.02	0.0025532
0.15	5.0959	0	0
0.1	3.1634	0.1	0.018723
0.075	1.9232	0.54	0.81872
0.05	1.1039	0.8	0.83234

Table A.2. Resolution test results for DS1

Scale	Decidability	FRR	FAR
1	7.9902	0	0
0.9	7.8999	0	0
0.8	7.5219	0	0
0.7	7.6782	0	0
0.6	8.4828	0	0
0.5	9.1576	0	0
0.4	8.4031	0	0
0.3	6.855	0	0
0.25	7.0282	0	0
0.2	6.8744	0	0
0.15	4.5021	0	0
0.1	2.8794	0.095238	0.021672
0.075	1.9525	0.42857	0.41176
0.05	0.79955	0.80952	0.86687

Table A.3. Resolution test results for DS2

Scale	Decidability	FRR	FAR
1	8.7986	0	0
0.9	9.0473	0	0
0.8	8.4822	0	0
0.7	8.8208	0	0
0.6	8.3602	0	0
0.5	9.1477	0	0
0.4	9.8358	0	0
0.3	8.1398	0	0
0.25	7.7585	0	0
0.2	7.4825	0	0
0.15	6.6958	0	0
0.1	3.3236	0.10526	0.090278
0.075	2.1504	0.31579	0.61979
0.05	1.6675	0.52632	0.93403

Table A.4. Resolution test results for DS3

Upphovsrätt

Detta dokument hålls tillgängligt på Internet — eller dess framtida ersättare — under 25 år från publiceringsdatum under förutsättning att inga extraordinära omständigheter uppstår.

Tillgång till dokumentet innebär tillstånd för var och en att läsa, ladda ner, skriva ut enstaka kopior för enskilt bruk och att använda det oförändrat för icke-kommersiell forskning och för undervisning. Överföring av upphovsrätten vid en senare tidpunkt kan inte upphäva detta tillstånd. All annan användning av dokumentet kräver upphovsmannens medgivande. För att garantera äktheten, säkerheten och tillgängligheten finns det lösningar av teknisk och administrativ art.

Upphovsmannens ideella rätt innehåller rätt att bli nämnd som upphovsman i den omfattning som god sed kräver vid användning av dokumentet på ovan beskrivna sätt samt skydd mot att dokumentet ändras eller presenteras i sådan form eller i sådant sammanhang som är kränkande för upphovsmannens litterära eller konstnärliga anseende eller egenart.

För ytterligare information om Linköping University Electronic Press se förlagets hemsida <http://www.ep.liu.se/>

Copyright

The publishers will keep this document online on the Internet — or its possible replacement — for a period of 25 years from the date of publication barring exceptional circumstances.

The online availability of the document implies a permanent permission for anyone to read, to download, to print out single copies for your own use and to use it unchanged for any non-commercial research and educational purpose. Subsequent transfers of copyright cannot revoke this permission. All other uses of the document are conditional on the consent of the copyright owner. The publisher has taken technical and administrative measures to assure authenticity, security and accessibility.

According to intellectual property law the author has the right to be mentioned when his/her work is accessed as described above and to be protected against infringement.

For additional information about the Linköping University Electronic Press and its procedures for publication and for assurance of document integrity, please refer to its www home page: <http://www.ep.liu.se/>